Title
Sheared Zonal Flow ExB Drifts Predicted from Emissive Probes and Measured by Laser-Induced Fluorescence

Journal
Contributions to Plasma Physics, 46(5-6)

ISSN
0863-1042

Authors
McWilliams, R
Edrich, D

Publication Date
2006-06-01

DOI
10.1002/ctpp.200610023

Contrib. Plasma Phys. **46**, No. 5-6, 411 – 415 (2006) / **DOI** 10.1002/ctpp.200610023

Sheared Zonal Flow ExB Drifts Predicted from Emissive Probes and Measured by Laser-Induced Fluorescence

R. McWilliams[*] and **D. Edrich**

Dept. of Physics and Astronomy University of California, Irvine, USA

Received 23 May 2005, accepted 14 September 2005
Published online 9 June 2006

Key words Emissive probes, ExB drift, Laser-induced fluoressence.
PACS 52.25.Fi, 52.70.Ds, 52.70.Kz, 52.38.-r, 52.25.Os

An electron beam sheet injected into a plasma created regions of oppositely-directed electric fields above and below the sheet. An emissive probe was used to measure the spatial structure of the plasma potential from which the electric field could be deduced. Laser-induced fluorescence (LIF) was used to measure the spatial structure of the ion zonal flow velocity. The ExB velocity flow field predicted from the emissive probe results is compared to the LIF observations.

1 Introduction

Since at least the time of Langmuir [1, 3], probes have been used to study basic plasma parameters including currents of the various species in plasmas. Emissive probes have found enduring utility in measuring the plasma potential [4]- [10]. Typically a non-emissive Langmuir probe may provide a measure of the probe floating potential when the collected electron and ion currents balance, from which the plasma potential may be estimated. There are no emitted currents in the usual cold Langmuir probe operation excepting secondary electron emission. Alternatively, the plasma potential may be estimated directly from properties around the knee of the I-V trace near the electron saturation current. Mach probes may provide [11]- [13] measures of plasma flows. An emissive probe has the benefit of providing a sea of electrons at the probe surface; these electrons may be emitted when the probe potential is negative compared to the plasma potential. Conceptually in terms of collected current, the emitted electrons act like a very low mass positive ion so the transition to ion saturation current may have a very steep slope on the I-V trace. The zero-current crossing-point potential for an emissive probe is easy to find and close to the actual plasma potential.

Plasma flows may be driven by spatial variation in the plasma potential. Of particular interest here is the ExB flow driven by steady-state plasma potential spatial variations. Zonal flows may be driven by plasma potential variations and shear in these flows may occur. Koepke, Carroll, and Zintl have reported [14] on instabilities formed with the production of zonal flows created in Q-Machine experiments by dc potential applications to the plasma-creating ionization plates and additional annulus/grid arrangements. They describe methods by which parallel (to B) and transverse velocity shear may be created. Their observations included the use of emissive probes for determining plasma potential (and inferring electric fields) and use of laser-induced fluorescence (LIF) for measuring ion distribution functions and flows. Typical electric field values were of the order of up to 250 V/m and ion flows up to 200 m/sec. Inhomogeneous energy-density driven instabilities were studied in these Q-Machine experiments with annular regions of flow shear.

Experiments reported here show dc potential structures created by the flow of an electron beam sheet down a magnetic field in an argon plasma. Emissive probes were used to measure the transverse potential variation near the beam sheet. Electric fields as high as 3000 V/m and ion flow velocities up to 250 m/sec were observed in a

[*] Corresponding author: e-mail: mcw@uci.edu

sheared zonal flow configuration around the beam sheet. The ion flows were measured with LIF. Comparison is made with the measured ion flow velocities and those predicted from the emissive probe measurements.

2 Experimental arrangement

The Irvine Torus [15] provided the test bed for these experiments. The vacuum vessel provides for a carbon limiter minor radius of the plasma of a=3.5 cm at a major radius of R=56.5 cm with toroidal magnetic field up to B=2 kG and typically run at 1 kG. There is no rotational transform. The sheet electron beam is produced by a 10 cm-long tungsten filament placed horizontally in the vacuum vessel. The filament is heated to thermionic emission of electron current of 0-1.5 amps (typically 100 mA) and biased (typically 300 volts) with respect to the vacuum chamber ground. Laplaces Equation in combination with the magnetic field means the emitted electrons are accelerated primarily parallel to the magnetic field and approach the bias potential (in the absence of plasma) in a toroidal distance of about 10 cm, the vacuum chamber minor radius. A background neutral argon pressure of up to 1 mTorr provides the gas for a small percentage ionization in the resulting discharge. Plasma densities, n, of $10^{10} - 10^{11} cm^{-3}$ are typical. Plasma electron temperatures are a few eV and the ions are near room temperature unless heating methods are employed which act in opposition to the ion-neutral charge-exchange cooling. Plasma electron and ion gyroradii are about ρ_e= 0.1 mm and ρ_i= 3 mm, respectively. The plasma Debye length is about λ_D= 0.3 mm. The electron beam energy is far above the plasma temperature, hence potentials associated with the electron beam are not expected to be shielded within a Debye distance. The experiments are performed at any location around the torus. Due to the localized nature of the experiment, the toroidal geometry is not thought to play an important role in the experiment. The geometry may be visualized as a Cartesian system locally with the sheet beam traveling down the z-axis and having major width of 10 cm extent in the x-direction. The geometry is shown in Figure 1.

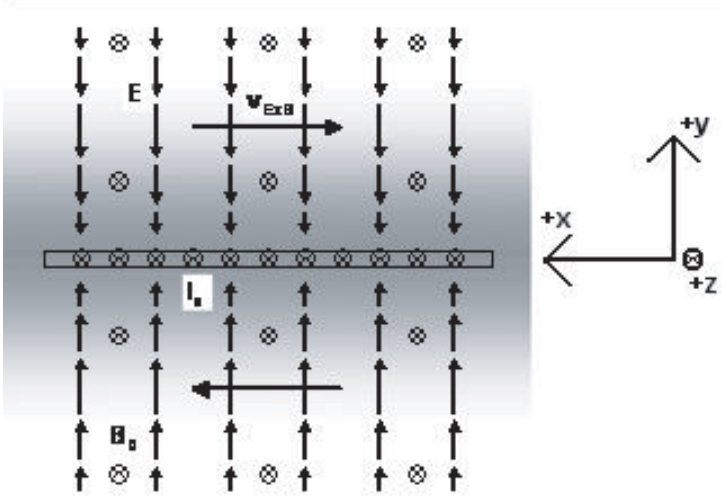

Fig. 1 Experiment geometry with magnetic field and electron beam sheet into the page.

Plasma density profiles and magnitudes may be measured with Langmuir probes. Plasma density also may be measured with lower hybrid waves. LIF is used for ion characterization [16]. Emissive probes were used for plasma potential measurements.

The propagation of the electron beam sheet down the magnetic field provides an excess negative charge in the region of the beam. As a result, an electric field is created which points downward towards the beam sheet from above and upwards towards the beam sheet from below. The y-direction extent of the electric field, how far it may reach vertically before being shielded by the plasma, provides a steady-state y-direction electric field which may cause ExB drift in the regions just above and below the beam sheet. The resultant ExB flow is expected in the x-direction. Because of the opposing directions of the electric field above and below the beam sheet, the ExB flows are expected to be oppositely directed above and below the beam sheet. These two adjacent zones of flow will have shear in the x-directed flow in the y-direction. The overall geometry and expected potential and electric field structures, along with the associated ExB flow may be visualized as shown in Figure 2.

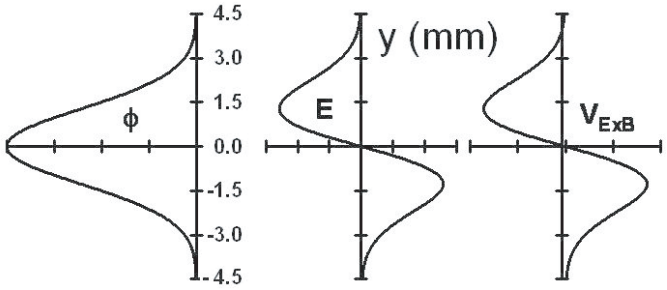

Fig. 2 Conceptual structure of the plasma potential, electric field and ion zonal flow in the vertical direction.

3 Experimental result

An emissive probe plasma potential scan versus y-direction is shown in Figure 3. The emissive probe was made as a half circle of 55-gauge tungsten wire curved to a 0.5 mm radius. The vertical position labeled 0 is at the center of the electron sheet beam. The primary feature is the dip in the plasma potential in the region of the beam. This dip has vertical extent, full width half maximum, of about 2.5 mm, about $10\lambda_D$. As with the Q-Machine experiments, the variation in plasma potential is up to around 3 volts. However, the transverse extent of the potential is now on the mm scale as opposed to the cm scale of the Q-Machine experiment. Hence, the electric fields inferred here from the plasma potential spatial variation are an order of magnitude higher than those reported in the Q-Machine experiments. These two experiments have rather different plasma and electric field formation circumstances yet some of the results are similar while some differ.

Next the dc electric fields were estimated from the derivative of plasma potential spatial variation measurements. These results are shown also in Figure 3 so the fields may be visualized with the potential structure. The electric field runs from 0 to a maximum of 3 kV/m in the example shown. The spatial extent of the electric field is around 2.5 mm, as expected from the potential structure. This distance scale is about 40% of a thermal ion Larmor diameter. Most ions sampling the electric field structure would not see a uniform electric field over the gyro-orbit as is often considered for ExB drift calculations. Rather, over an orbit an ion will see an electric field varying from nothing up to the maximum (if it travels through that region) with an average electric field much less than the maximum value. Now imagine different classes of ions based on their orbits.

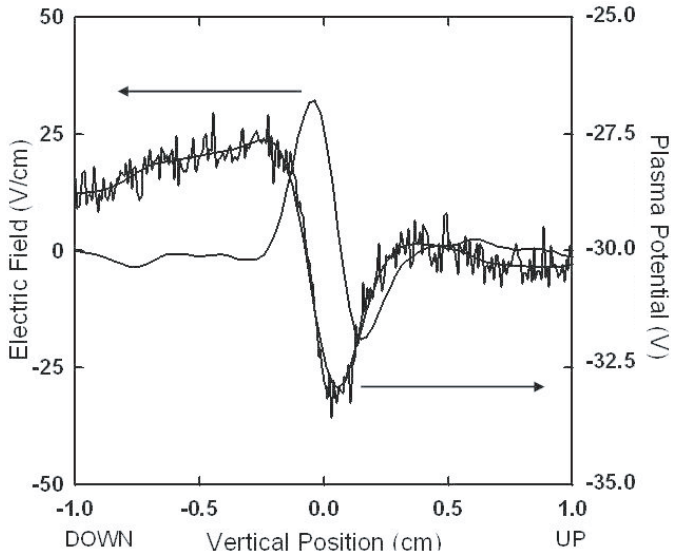

Fig. 3 Plasma potential as a function of vertical position along with the inferred electric field.

Consider first an ion above the electron beam sheet which has a Larmor orbit sufficiently above the sheet that it just samples the electric field along the bottom edge of its Larmor orbit. Such an ion will have negligible ExB drift since its orbit is perturbed by the electric field very little. The increase in Larmor orbit would be followed promptly by a decrease in the orbit. Hence, little lateral ExB motion can occur.

The ion class which might be expected to have the largest ExB excursion per orbit would be the ions with Larmor orbit centered on one of the electric field peaks. For example, consider an ion centered on the larger-E peak of Figure 3. This ion will receive a 3 eV energy boost when passing through the electric field. The ion started initially with a 2.9 mm gyro-radius which now is boosted up to 1.6 cm gyro-radius. In a uniform electric field, one would expect this ion to carry a large gyro-radius until reversing direction, whereupon the gyro-radius will decrease again by the 3 eV drop in energy. The net lateral motion occurs due to uneven gyro-radius over the full gyro-period. However, in the present case, the ion now has a large enough gyro-orbit to sample the oppositely-directed electric field on the opposing side of the electron beam sheet. And it does this sampling within a small extent of the 3 eV, 1.6 cm gyro-orbit. The net result is nearly-canceling electric field kicks in terms of ExB-induced motion; the net effect is about $1/10^{th}$ the ExB drift expected alone from the electric field peak on which this class of ion is centered. It is easy to see that the factor must be a reduction from the peak-E for the net ExB drift because of the opposing effects of the two regions of electric field. That the factor is $1/10^{th}$ comes from numerical simulation of the ion orbit for the plasma parameters of Figure 3. Thus, the ion ExB drift is expected to range from zero to about $1/10^{th}$ the estimate from a single electric field peak region depending on the class of ion (i.e., the ions initial energy and gyro-center).

As a rough estimate of the kick expected from a single electric field peak (without the canceling from the other peak), an ion with Larmor orbit centered on the peak of the electric field would see a 3 eV boost on passing through the electric field region in one direction and a 3 eV deceleration on passing the opposite way. The boost results in an ExB drift of $2.4 \times 10^3 m/s$ in the x-direction if the other peak is not sampled. However, any ion which samples the peak region will be boosted enough to sample the opposing field peak region as well.

Hence, nearly all ions on one side of the electron beam sheet will have a net ExB drift induced which is about $1/10^{th}$ the value just cited, i.e. ions are predicted to ExB drift at about 240 m/s in the x-direction. The ions centered on the electric field peak on the opposite side of the electron sheet beam will have a similar drift speed but in the opposite x-direction. The expected ExB drift would be reduced further by charge exchange losses which are estimated to occur with a mean free path of 5 cm for these experiments and thus probably is a small reduction.

Once the region of the electric field structure was identified, laser-induced fluorescence could be brought to bear to find the ion drift velocities. The LIF equipment used had a spatial resolution of about 1 mm in the y-direction. A horizontal LIF beam launched along the x-axis at various y-positions (vertical) thus could give the ion flow field as a function of position above and below the electron beam sheet. The LIF is absolutely calibrated with an iodine reference cell. The results are shown in Figure 4. Here we see first that there is a variation in ion convective flow above and below the beam sheet. The ion flow is in the direction of the expected ExB drifts. There are two zones of oppositely-directed flow with a sheared region between. The maximum ion drift

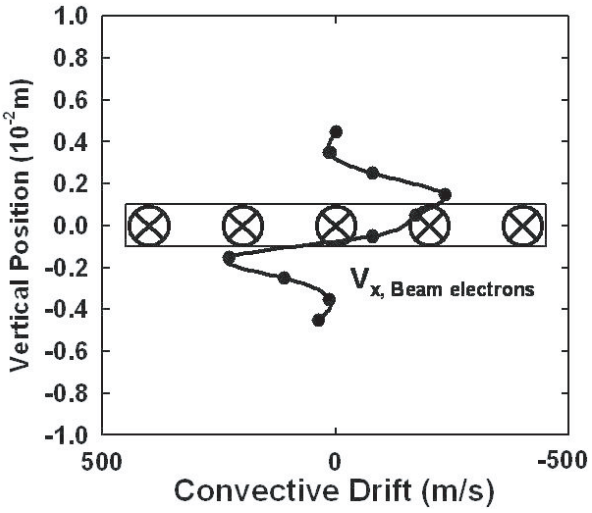

Fig. 4 Ion convective flow velocities in the horizontal direction as measured by LIF. Random error in convective drift speed analysis approximately size of data symbols.

velocities measured were about 250 m/sec. Considering the y-profile of the observed ion flow in the x-direction along with the 1 mm laser beam waist and Gaussian intensity profile in that beam waist, the peak ion flow velocity is estimated to be about 281 m/sec at the maximum flow position where the 250 m/sec is average collected over

the laser excitation volume. The peak ion flow speed estimated from the LIF is 15% above the rough prediction based on the emissive probe measurements. At this level of estimation, the emissive probe predictions are born out by the LIF observations.

Beyond the basic plasma physics of this experiment, these results may be set in the context of applied plasma physics in tokamak fusion research. Zonal flow is a topic of interest in tokamaks. Sheared flow is thought to be a possible mechanism for suppression of turbulence (and therefore undesirable transport) in tokamaks. For the results of Figure 4, we see a shear rate in the ion flow of about $2 \times 10^5 sec^{-1}$. This is precisely the shear estimated for the D-III tokamak [17]. We also note the electric fields observed here are comparable to the radial fields observed [18] in tokamak scrape-off layers during QH-mode operation with internal transport barriers (ITB). And we note that the adjacent zonal flow regions interact with each other resulting in reduced convective flow magnitudes in each zone because of the nonlocal sampling by the ions of the neighboring electric field structures in the zones of opposing flow.

Acknowledgements Supported by NSF Grant INT-9981978 and DoE Grant DE-FG03-99ER54542

References

[1] K. Compton and I. Langmuir, Rev. Mod. Phys. **2**, 123 (1930).
[2] I. Langmuir and K. Compton, Rev. Mod. Phys. **3**, 954 (1931).
[3] I. Langmuir, Phys. Rev. **33**, 954 (1933).
[4] R. Kemp and J. Sellen, Rev. Sci. Instrum. **37**, 455 (1966).
[5] H. Yamada and D. Murphree, Phys. Fluids **14**, 1120 (1971).
[6] N. Hershkowitz et al., Rev. Sci. Instrum. **54**, 29 (1983).
[7] N. Hershkowitz and M. Cho, J. Vac. Sci. Technol. **A6**, 2054 (1988).
[8] M. Ye and S. Takamura, Phys. Plasmas **7**, 3457 (2000).
[9] R. Schrittwieser, et al., Plasma Phys. Control. Fusion **44**, 567 (2002).
[10] W. Amatucci et al., Phys. Plasmas **11**, 2097 (2004).
[11] K.-S. Chung, et al., Phys. Fluids B **1**, 2229 (1989).
[12] I. Hutchinson, Plasma Phys. Control. Fusion **44**, 1953 (2002).
[13] L. Oksuz and N. Hershkowitz, Plasma Sources Sci. Technol. **13**, 263 (2004).
[14] M. Koepke, J. Carroll, and M. Zintl, Phys. Plasmas **5**, 1671 (1998).
[15] R. McWilliams and R. Platt, Phys. Rev. Lett. **56**, 835 (1986).
[16] G. Severn, D. Edrich, and R. McWilliams, Rev. Sci. Instrum. **69**, 10 (1998).
[17] S. Coda, M. Porkolab, and K.H. Burrell, Phys. Rev. Lett. **86**, 4835 (2001).
[18] E.J. Doyle, et al., Plasma Phys. Contr. Fusion, **43**, A95 (2001).

